

Slow and Fast Transitions in the Rising Phase of Outbursts from NS-LMXB transients, Aql X-1 and 4U 1608–52

Kazumi ASAI,¹ Masaru MATSUOKA,¹ Tatehiro MIHARA,¹ Mutsumi SUGIZAKI,¹ Motoko SERINO,¹ Satoshi NAKAHIRA,¹ Hitoshi NEGORO,² Yoshihiro UEDA,³ and Kazutaka YAMAOKA⁴

¹MAXI team, RIKEN, 2-1 Hirosawa, Wako, Saitama 351-0198

kazumi@crab.riken.jp

²Department of Physics, Nihon University, 1-8-14 Kanda-Surugadai, Chiyoda-ku, Tokyo 101-8308

³Department of Astronomy, Kyoto University, Kitashirakawa, Oiwake-cho, Sakyo-ku, Kyoto 606-8502

⁴Department of Physics and Mathematics, Aoyama Gakuin University, 5-10-1 Fuchinobe, Chuo-ku, Sagami-hara 252-5258

(Received 2012 February 25; accepted 2012 June 18)

Abstract

We analyzed the initial rising behaviors of X-ray outbursts from two transient low-mass X-ray binaries (LMXBs) containing a neutron-star (NS), Aql X-1 and 4U 1608–52, which are continuously being monitored by MAXI/GSC in 2–20 keV, RXTE/ASM in 2–10 keV, and Swift/BAT in 15–50 keV. We found that the observed ten outbursts are classified into two types by the patterns of the relative intensity evolutions in the two energy bands below/above 15 keV. One type behaves as the 15–50 keV intensity achieves the maximum during the initial hard-state period and drops greatly at the hard-to-soft state transition. On the other hand, the other type does as both the 2–15 keV and the 15–50 keV intensities achieve the maximums after the transition. The former have the longer initial hard-state ($\gtrsim 9$ d) than the latter's ($\lesssim 5$ d). Therefore, we named them as slow-type (S-type) and fast-type (F-type), respectively. These two types also show the differences in the luminosity at the hard-to-soft state transition as well as in the average luminosity before the outburst started, where the S-type are higher than the F-type in the both. These results suggest that the X-ray radiation during the pre-outburst period, which heats up the accretion disk and delays the disk transition (i.e., from a geometrically thick disk to a thin one), would determine whether the following outburst becomes S-type or F-type. The luminosity when the hard-to-soft state transition occurs is higher than $\sim 8 \times 10^{36}$ erg s⁻¹ in the S-type, which corresponds to 4% of the Eddington luminosity for a 1.4 M_{\odot} NS.

Key words: Stars: neutron — X-rays: binaries — X-rays: individual (Aql X-1, 4U 1608–52) — X-rays: transients

1. Introduction

Soft X-ray transients (SXTs) are a group of X-ray binary systems that occasionally exhibit bright outbursts in a soft X-ray band. They are mostly identified as a low-mass X-ray binary (LMXB) containing either a neutron-star (NS-LMXB) or a black hole (BH-LMXB). The luminosity of the NS-LMXBs increases by 2–5 orders of magnitude during the outbursts. As the luminosity increases, the spectral state usually changes from the low/hard state to the high/soft state in both the NS-LMXB and the BH-LMXB (e.g., van der Klis 1994; Campana et al. 1998; Remillard & McClintock 2006). The low/hard state has a low intensity and a very hard spectrum, where the Comptonized component is dominant. On the other hand, the high/soft state has a high intensity and a very soft spectrum, where the thermal component is dominant. We study the initial rising phases of the NS-LMXB outbursts in this paper.

NS-LMXBs have been classified into two groups, Z sources and Atoll sources, based on the behavior on the color-color diagram (Hasinger & van der Klis 1989). Z sources are generally bright and sometime become close to

the Eddington luminosity limit. On the other hand, Atoll sources are generally less bright, and some of them show transient activity. The luminosity changes by three order of magnitudes from the quiescent state to the active state, whose luminosity also reaches close to the Eddington limit at the maximum. Homan et al. (2010) suggested that the differences between Z and Atoll sources are originated from the mass accretion rate.

The hard-to-soft state transition in the Atoll sources is also mainly due to the mass accretion rate. However in some transient objects, the mass accretion rate is not the only parameter that determines the hard-to-soft state transition (Yu & Dolence 2007; Yu et al. 2004; Smith et al. 2002; Homan et al. 2001). Therefore, it has not been completely understood which parameter actually derives the hard-to-soft state transition.

The hard-to-soft transition in the rising phase and the soft-to-hard transition in the decay phase have been studied separately. Yu and Yan (2009) and Tang, Yu, and Yan (2011) analyzed the relation of the X-ray luminosity at the hard-to-soft transition to the peak luminosity during the subsequent soft state as well as to the luminosity-increasing rate at the transition in both the NS-LMXBs

and the BH-LMXBs of both the transients and the persistents. They concluded from the results that the hysteresis between the hard-to-soft and the soft-to-hard state transitions is primarily due to a non-stationary accretion flow when mass-accretion rate increases. Maccarone (2003) reported that the soft-to-hard transition in the decay phase occurs at a luminosity of 1%–4% of the Eddington limit. Maccarone and Coppi (2003) suggested that the propeller mechanism is not the sole cause for the state transition in NS-LMXBs from the results of RXTE observations of Aql X-1, which showed that the luminosity in the hard-to-soft transition in the rising phase is greater than that in the soft-to-hard transition by a factor of ~ 5 or more. Such a hysteric behavior was first pointed out by Miyamoto et al. (1995) for the rising phase of BH-LMXBs.

X-ray spectra of NS-LMXBs basically show a monotonous continuum. However, the emission model is still controversial because they exhibit complex time variations linked with the change of the spectral states. A variety of spectral models have been proposed so far to explain their entire behaviors with a unified scheme. They are represented by two major models, the Eastern model (after Mitsuda et al. 1984, 1989) and the Western model (after White et al. 1988). These models generally consist of two components, a blackbody radiation with one or more temperatures and a Comptonized radiation extending to the hard X-ray band (Barret 2001; Gierliński & Done 2002; Lin et al. 2007; Farinelli et al. 2008; Takahashi et al. 2011; Sakurai et al. 2012). In the high/soft state, the blackbody radiation is dominant where the Comptonized radiation still exists in the low level (Gierliński & Done 2002; Paizis et al. 2006; Lin et al. 2007; Raichur et al. 2011). The Comptonized component is pointed out to be a major component in the low/hard state (e.g., Mitsuda et al. 1989). The site of the high-energy electrons responsible for the Comptonization and the seed photons are still a source of arguments.

4U 1608–52 and Aql X-1 are famous transient NS-LMXBs, where Type I X-ray bursts have also been detected in both sources (4U 1608–52: Nakamura et al. 1989, Aql X-1: Koyama et al. 1981). Their outbursts typically show a sharp rise and an exponential decay. Campana et al. (1998) reported that the rise time is 5–10 d and the exponential decay time is 30–70 d in Aql X-1, and also that 4U 1608–52 sometimes occurs outbursts with a symmetric evolution between the rise and the decay. The periodicity of the outbursts has been reported in both 4U 1608–52 (e.g., Šimon 2004) and Aql X-1 (Kitamoto et al. 1993; Šimon 2002). Chen, Zhang, and Ding (2006) reported that 4U 1608–52 occurs the soft-to-hard transition when the luminosity is in $(3.3\text{--}5.3)\times 10^{36}$ ergs s^{-1} , assuming that the distance to the source is 3.6 kpc. As for Aql X-1, it is reported that the hard-to-soft transition occurs at the luminosity of $(4.2\text{--}5.5)\times 10^{36}$ ergs s^{-1} and the soft-to-hard transition at $(6.1\text{--}7.5)\times 10^{35}$ ergs s^{-1} assuming the distance of 2.5 kpc (Maccarone & Coppi 2003; Maccarone 2003).

In this paper, we focus on the behaviors of the rising phase of outbursts from 4U 1608–52 and Aql X-1. We

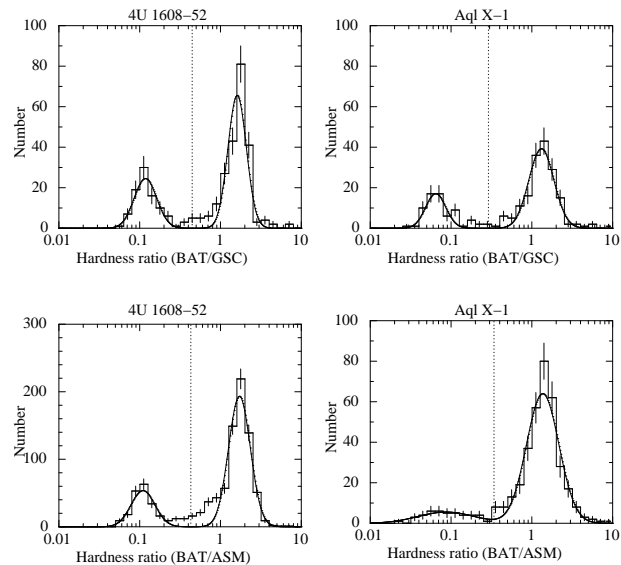


Fig. 1. Distributions of hardness ratios of BAT/GSC (top) and BAT/ASM (bottom) on a one-day timescale for 4U 1608–52 (left) and Aql X-1 (right), where the vertical error bars represent 1- σ statistical uncertainty. The best-fit model of two log-normal distributions are overlaid. The vertical dotted lines represent the thresholds between the soft and the hard states which we adopted.

investigate the evolution of their spectral states using the X-ray light curves and the hardness ratio obtained from the data of continuous monitoring with MAXI/GSC in 2–20 keV, RXTE/ASM in 2–10 keV, and Swift/BAT in 15–50 keV. We classify all observed outbursts by the pattern of the state transition during the rising phase. We then analyze their differences and discuss what determines the different evolution patterns. We employ the distances of 4.1 ± 0.4 kpc for 4U 1608–52 and that of 5.0 ± 0.9 kpc for Aql X-1 following Galloway et al. (2008) hereafter throughout the paper.

2. Analysis and Results

2.1. MAXI-GSC, Swift-BAT Light Curves and the Hardness Evolution

MAXI (Monitor of All-sky X-ray Image: Matsuoka et al. 2009) on the International Space Station (ISS) started the all-sky survey on 2009 August 15 with GSC (Gas Slit Camera: Mihara et al. 2011; Sugizaki et al. 2011a) in 2–30 keV and SSC (Solid-state Slit Camera: Tomida et al. 2011) in 0.5–12 keV. The GSC with MAXI nova alert system (Negoro et al. 2010) has detected two outbursts from 4U 1608–52 in 2010 March (Morii 2010) and in 2011 March (Sugizaki et al. 2011b) and three outbursts from Aql X-1 in 2009 November, 2010 September, and 2011 October (Yamaoka et al. 2011). We obtained the GSC light curve data in 2–20 keV band from the public archive¹ provided by MAXI team. We also obtained the light-curve data in the hard X-ray band of 15–50 keV

¹ <<http://maxi.riken.jp/>>.

monitored by BAT (Burst Alert Telescope: Barthelmy et al. 2005) on board Swift (Gehrels et al. 2004) from the transient-monitor results provided by the Swift-BAT team.²

We identified the spectral state from the BAT/GSC hardness ratio using the same method employed in Yu and Yan (2009) and Tang, Yu, and Yan (2011). X-ray spectra of both 4U 1608–52 and Aql X-1 can be approximated by a two-component model consisting of a blackbody emission and a Comptonized emission (figure 2 in Gierliński & Done 2002 for 4U 1608–52 and figure 5 in Lin et al. 2007 for Aql X-1). In the soft state, the blackbody emission with a temperature of $kT \simeq 0.5\text{--}2.0$ keV becomes significant and dominates the GSC 2–20 keV band. Meanwhile, the flux in the BAT band of 15–50 keV are mostly dominated by the Comptonized emission which often extends to several tens keV. Therefore, the ratio represents the spectral state.

To determine the best threshold to discriminate the two states, we investigated the distributions of the daily hardness ratio of the BAT 15–50 keV flux to the 2–20 keV GSC flux as shown in figure 1. The fluxes are converted to that in Crab unit using the nominal Crab values of $3.6 \text{ photons s}^{-1} \text{ cm}^{-2}$ in the GSC (cf. footnote 1) and $0.22 \text{ counts s}^{-1} \text{ cm}^{-2}$ in the BAT (cf. footnote 2). We used all of the data points obtained from 2009 August 15 (MJD=55058) to 2011 December 19 (MJD=55914) after MAXI started the all-sky survey. The distributions of both 4U 1608–52 and Aql X-1 clearly show two peaks corresponding to the soft and the hard states. We fitted the histogram with a model of two log-normal distributions and determined the soft-hard threshold at the center of the two peaks obtained from the best-fit parameters. The center values of the Gaussian (C_1 and C_2) are $\log_{10} C_1 = 0.21 \pm 0.02$, $\log_{10} C_2 = -0.93 \pm 0.03$ and $\log_{10} C_1 = 0.12 \pm 0.02$, $\log_{10} C_2 = -1.19 \pm 0.04$, for 4U 1608–52 and Aql X-1, respectively. The obtained thresholds, $10^{(\log_{10} C_1 + \log_{10} C_2)/2}$, are 0.44 and 0.29, respectively.

Figure 2 shows GSC light curves, BAT light curves, and the hardness ratios (BAT/GSC) for the five outbursts. First, we estimated the outburst onset from the GSC light curve with a 1-day time bin. The archived GSC light-curve data include a systematic error of $\sim 5\text{mCrab}$ for the imperfection in the background subtraction. We confirmed that the systematic error does not affect the results of the following analysis significantly. Once outbursts started, the flux increased steadily from nominal low level below 10 mCrab towards the peak over 100 mCrab. When the trend of source luminosity before outburst onset was constant or decreasing, the outburst onset can be determined clearly. When the source luminosity before outburst onset was increasing, we determine the onset in the following way. The outburst typically shows a sharp exponential rise, whose slope is different from the persistent component. However, the rise curve sometimes has more than one slope even in the rising period, then we can-

not determine the onset just by the changing point of the slopes. Therefore in this paper, we define the outburst onset as the start-point of the increase trend towards the peak. In order to determine the start-point, we fitted light curves around the outburst onset with two exponential functions, and define the “cross point” of the two exponential functions as the start-point of the outburst. The results are shown in the Appendix.

We next estimate the time and the luminosity when the hard-to-soft transition occurs from data bins of the “last hard state” and the “first soft state”. We employed the center of two data bins as “transition time (time when transition occurs)” and their time interval as the error on it. We also defined their average luminosity as the “transition luminosity”. Thus, the “pre-transition time” is defined by the duration from the “outburst onset” to the “transition time”. The derived epoch of the “outburst onset”, “pre-transition time”, and “transition luminosity” for each outburst are summarized in table 1.

To inspect the relative intensity variations between the GSC and the BAT bands, GSC–BAT intensity–intensity diagrams from 10 d before the outburst onset to the end of the soft state are plotted in figure 3, where fluxes in the GSC and BAT light curves are converted to the luminosities in the 2–15 keV and in the 15–50 keV, respectively, assuming that the spectrum is Crab-like (Kirsch et al. 2005).

These intensity–intensity diagrams are obviously classified into two types. One type behaves as the two intensities in the different energy bands of 2–15 keV and the 15–50 keV become the maximum almost simultaneously in the soft state after the hard-to-soft transition occurred (figures 3a, 3b). The other type behaves as the 15–50 keV intensity reaches the maximum earlier than the 2–15 keV intensity (figures 3c, 3d, 3e). Then, the 15–50 keV intensity during the soft state does not exceed the maximum just before the hard-to-soft transition state, whereas the 2–15 keV intensity reaches its maximum after the hard-to-soft transition. These two types are apparently related with the pre-transition time as shown in table 1. The pre-transition time is shorter than 5 d in the former type but longer than 9 d in the latter type for the five outbursts observed by GSC. We therefore name the former as Fast(F)-type and the latter as Slow(S)-type.

2.2. RXTE-ASM, Swift-BAT Light Curves and the Hardness Evolution

To confirm the results obtained from the MAXI-GSC and Swift-BAT light curves in the previous subsection, we also analyzed outbursts from the same sources observed with the ASM (All Sky Monitor: Levine et al. 1996) in-board RXTE (Rossi X-ray Timing Explorer: Bradt et al. 1993) in 2–10 keV. The ASM data are obtained from the archived results provided by the RXTE-ASM teams at MIT and NASA/GSFC.³ We found four outbursts from 4U 1608–52 and one outburst from Aql X-1 since the Swift started the operation in 2004 November until the

² <<http://heasarc.gsfc.nasa.gov/docs/swift/results/transients/>>.

³ <<http://xte.mit.edu/>>.

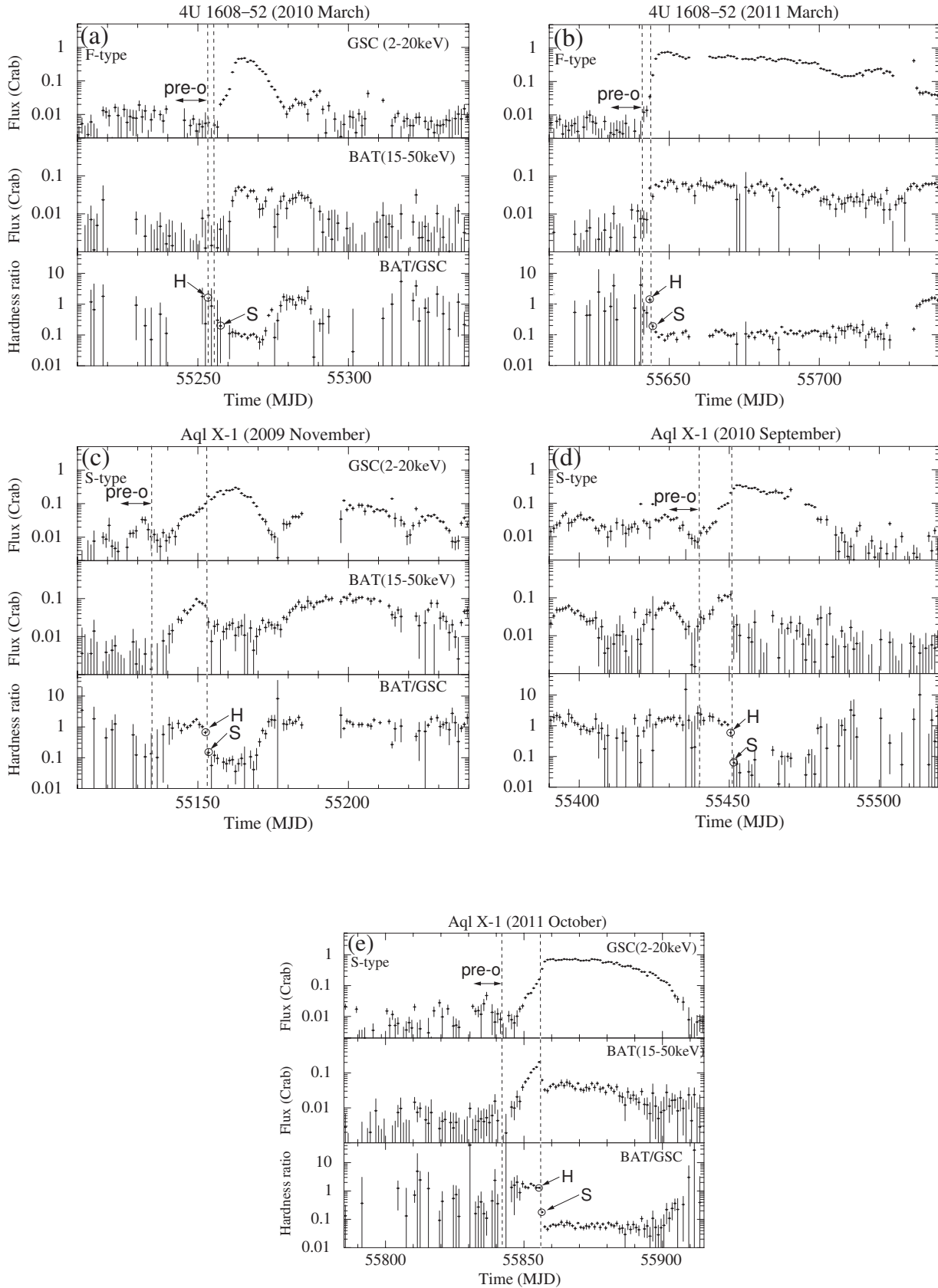


Fig. 2. MAXI-GSC light curves (2–20 keV), Swift-BAT light curves (15–50 keV), and the hardness ratios (BAT/GSC) of five outbursts. The vertical error bars represent $1\text{-}\sigma$ statistical uncertainty. The labels “H” and “S” are defined in subsection 2.1 as the last point of the hard state and the first point of the soft state, respectively. The two vertical dashed lines indicate the time at the outburst onset (left) and that at the hard-to-soft transition (right) that we derived. The “pre-o” denotes the pre-outburst period used in subsection 2.3, which is 10 d before the outburst onset.

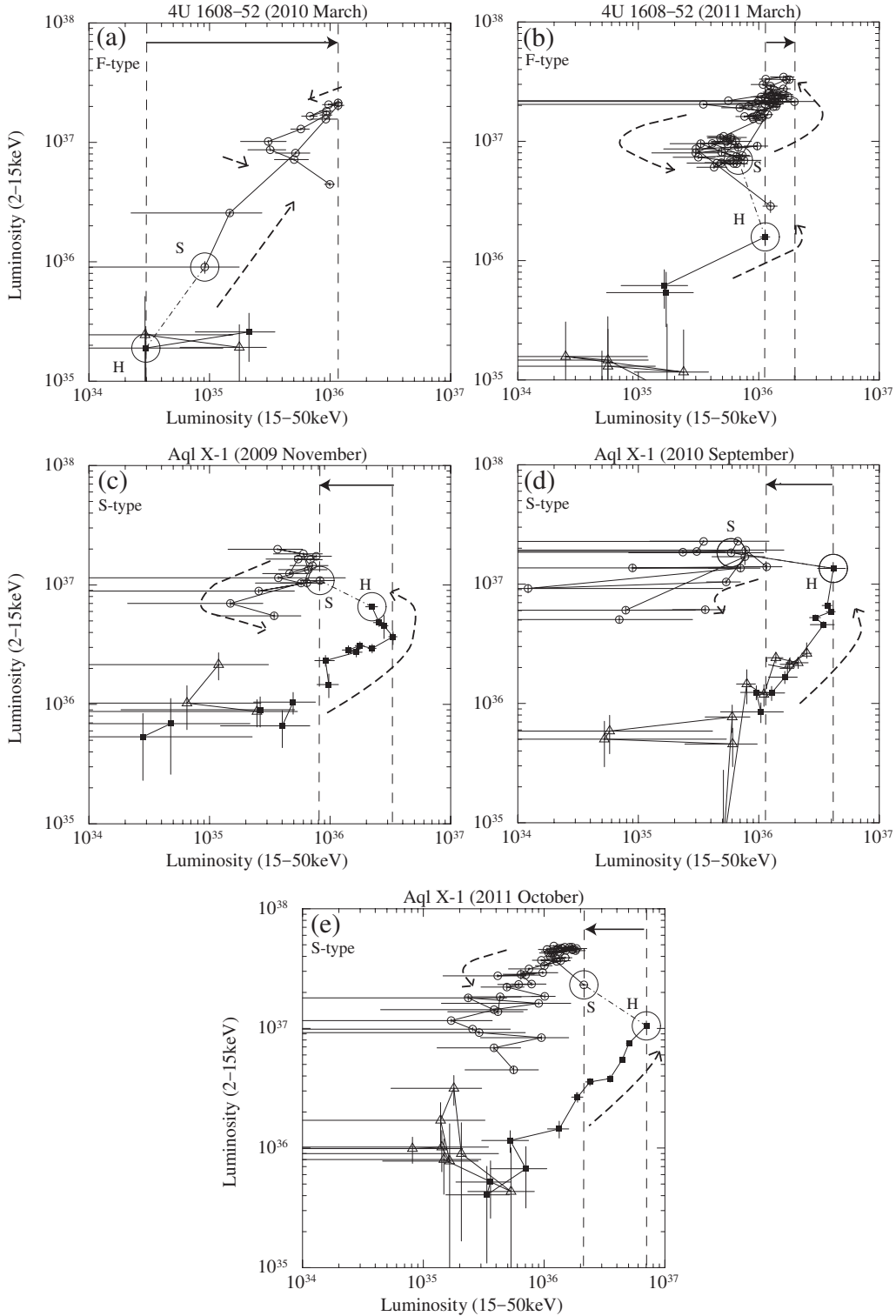


Fig. 3. GSC (2–15 keV) and BAT (15–50 keV) intensity–intensity diagram. Error bars represent $1\text{-}\sigma$ statistical uncertainties. Open triangles, filled squares, open circles represent data before the outburst start, during the initial hard state, and during the soft state, respectively. Furthermore, we connected the data points in the same state along the time evolution. Labels of “H”, and “S” represent the data at just before/after the hard-to-soft transition (H and S) with the dash-dot line. The dashed lines with arrows indicate the time sequence of each outburst. The two vertical dashed lines indicate the 15–50 keV peak luminosities during each hard/soft state. The top horizontal arrow indicates the direction of the change from the hard state to the soft state.

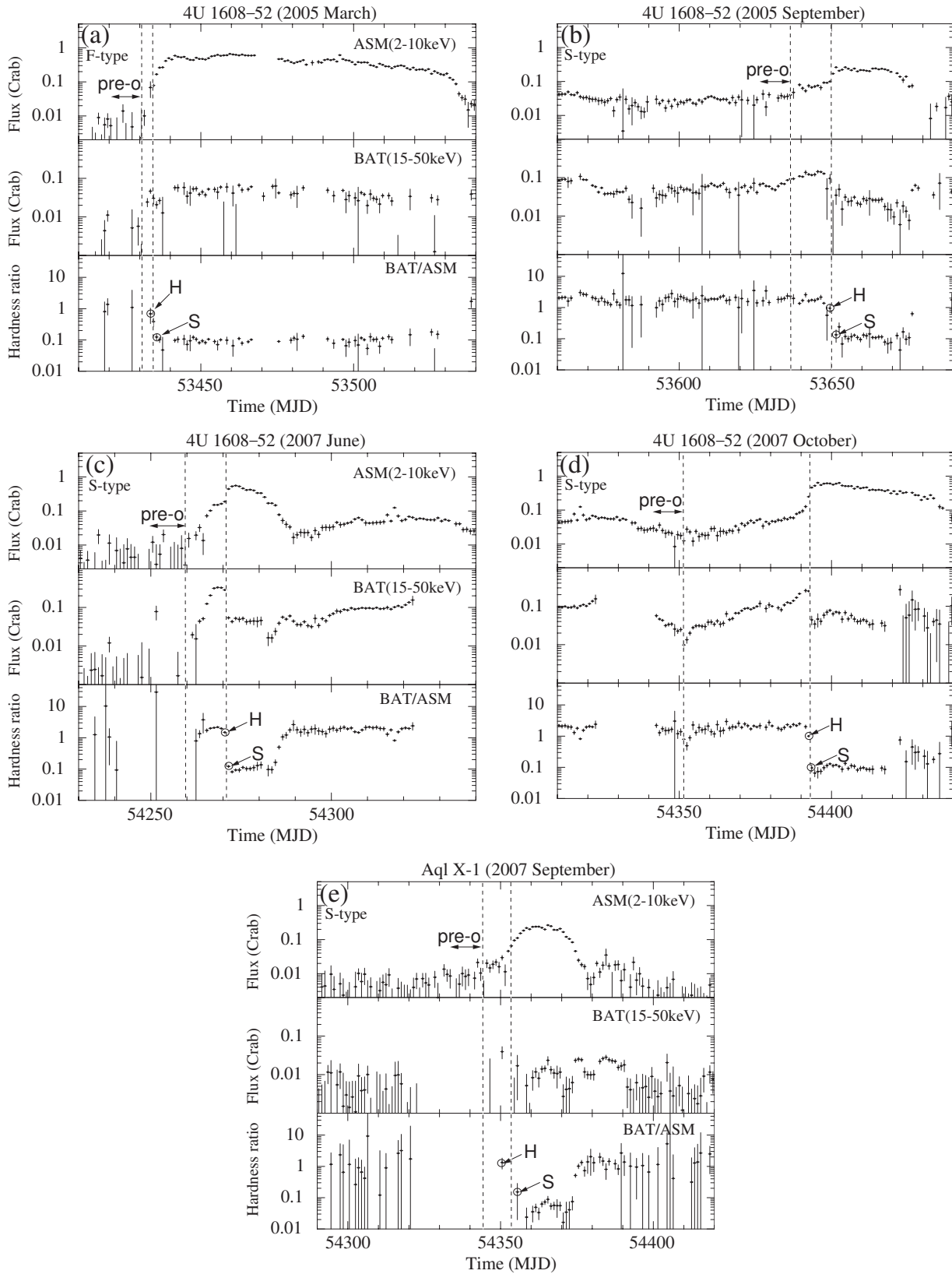


Fig. 4. RXTE-ASM light curves (2–10 keV), Swift-BAT light curves (15–50 keV), and the hardness ratios (BAT/ASM) of five outbursts. The labels and errors are the same as in figure 2.

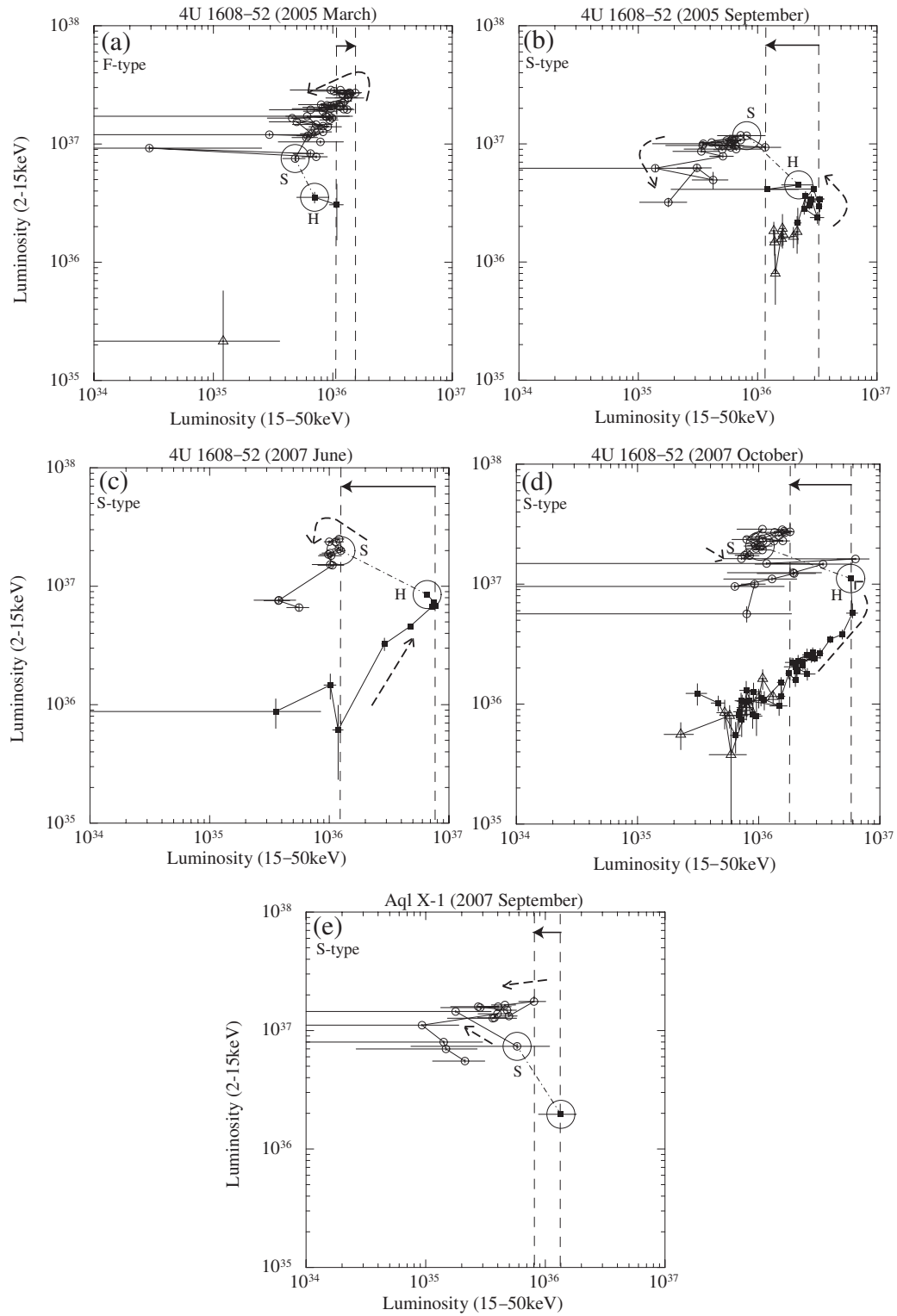


Fig. 5. Same as figure 3, but using ASM and BAT data.

Table 1. Parameters of five outbursts observed by MAXI/GSC and Swift/BAT.

	4U 1608–52		Aql X-1		
	(2010 Mar)	(2011 Mar)	(2009 Nov)	(2010 Sep)	(2011 Oct)
Outburst onset * (MJD)	55253.5 ± 0.5	$55641.5^{+0.8}_{-0.6}$	55134.4 ± 0.6	55440.7 ± 1.0	$55842.2^{+1.0}_{-0.7}$
Transition time [†] (MJD)	55255.5 ± 2.0	55644.0 ± 0.5	55153.0 ± 0.5	55451.0 ± 0.5	55856.0 ± 0.5
Last hard state					
time [‡] (MJD)	55253.5 ± 0.5	55643.5 ± 0.5	55152.5 ± 0.5	55450.5 ± 0.5	55855.5 ± 0.5
Hardness ratio [§]	2 ± 1	1.3 ± 0.2	0.66 ± 0.08	0.6 ± 0.1	1.30 ± 0.07
Luminosity ^l	0.03 ± 0.01	0.16 ± 0.02	0.66 ± 0.03	1.35 ± 0.04	1.05 ± 0.04
First soft state					
time [‡] (MJD)	55257.5 ± 0.5	55644.5 ± 0.5	55153.5 ± 0.5	55451.5 ± 0.5	55856.5 ± 0.5
Hardness ratio [§]	< 0.4	0.19 ± 0.04	0.15 ± 0.05	0.06 ± 0.05	0.18 ± 0.01
Luminosity ^l	0.09 ± 0.01	0.69 ± 0.05	1.09 ± 0.07	1.83 ± 0.05	2.31 ± 0.05
Pre-transition time [#] (days)	3.5 ± 1.0	$2.5^{+1.1}_{-1.3}$	18.6 ± 1.1	10.3 ± 1.5	$13.8^{+1.2}_{-1.5}$
Transition luminosity ^{**}	0.06 ± 0.03	0.4 ± 0.3	0.9 ± 0.2	1.6 ± 0.2	1.7 ± 0.6
Soft/Hard state at 15–50 keV max. ^{††}	soft state	soft state	hard state	hard state	hard state
Type	F	F	S	S	S

* See the Appendix.

[†] The “transition time” is defined by the middle of the “last hard state” and the “first soft state”, and the error is defined by the span between the both data points.

[‡] All errors of the “time [MJD]” are ± 0.5 d, indicating that the data points are for 1-day average.

[§] Hardness ratio means 15–50 keV/2–15 keV.

^l Luminosity in 2–15 keV band in the unit of 10^{37} erg s⁻¹. The errors in “Luminosity” are 1- σ errors.

[#] “Pre-transition time” means the initial hard-state duration from “Outburst onset” to the “Transition time”.

^{**} “Transition luminosity” is an average luminosity from “Last hard state” to “First soft state” in 2–15 keV band in unit of 10^{37} erg s⁻¹.

^{††} Whether soft state or hard state when the 15–50 keV luminosity reached the maximum.

MAXI started in 2009 August. We performed the same analysis procedure as applied for the GSC and BAT data in the previous subsection. Figure 4 shows the ASM light curves in 2–10 keV, the BAT light curves in 15–50 keV, and the hardness ratios of BAT/ASM for the five outbursts, where ASM data are converted to a flux in Crab unit using the nominal relation of 1 Crab = 75 counts s⁻¹ for ASM.⁴

We also examined the hardness-ratio distribution as has been shown in figure 1. We used all of the data points obtained from 2005 February 13 (MJD=53414) to 2011 July 31 (MJD=55773) after Swift started the operation. We fitted the histogram with a model of two log-normal distribution functions and determined the soft-hard threshold at the center of the two peaks obtained from the best-fit parameters. The center values of the Gaussian (C_1 and C_2) are $\log_{10} C_1 = 0.23 \pm 0.01$, $\log_{10} C_2 = -0.96 \pm 0.02$ and $\log_{10} C_1 = 0.13 \pm 0.02$, $\log_{10} C_2 = -1.1 \pm 0.2$, for 4U 1608–52 and Aql X-1, respectively. The obtained thresholds $10^{(\log_{10} C_1 + \log_{10} C_2)/2}$, are 0.43 and 0.34, respectively. Figure 5 shows the ASM–BAT intensity–intensity diagrams representing the relations between the 2–15 keV and the 15–50 keV intensities from 10 d before the outburst onset to the end of the soft state. In the outburst of 4U 1608–52 in 2007 October (figure 4), a large flux increase in the 15–50 keV band was observed in the soft state, which seems to be the second peak in the BAT band.

Table 2 summarizes the parameters of the five outbursts

by ASM and BAT obtained in the same manner as in table 1.

Since the Aql X-1 outburst in 2007 September has a large data gap in the BAT data around the “transition time (MJD)”, “pre-transition time (days)” has large errors. All the obtained results confirmed that the outbursts detected by ASM also show the same features of either S-type or F-type as seen in the five outbursts detected by GSC as described in subsection 2.1. The pre-transition times in the F-types are shorter than that in the S-type.

2.3. Relation of Pre-outburst Luminosity, Transition Luminosity on Transition Behavior

To find the root causes for the two behaviors of S-type and F-type, we here investigate parameters that have a correlation with the pre-transition time.

Firstly, we examined the source luminosities before the outburst onset. The source luminosities before the outburst onsets changed more than one order of magnitude in several time scales (5–100 d) even in the quiescent phase. In calculating “pre-outburst luminosity”,⁵ we adopted 10 d interval, which according to average transition time

⁵ We adopted all the public data of MAXI/GSC and RXTE/ASM through the present analysis. However, the weaker intensities probably include some background component. Thus “pre-outburst luminosities” for the F-types may be contaminated with the background component considerably and may be upper limit. Nevertheless, the present conclusion is not affected.

⁴ <http://xte.mit.edu/XTE/ASM_lc.html>.

Table 2. Parameters of five outbursts observed by RXTE/ASM and Swift/BAT.*

	4U 1608–52				Aql X-1
	(2005 Mar)	(2005 Sep)	(2007 Jun)	(2007 Oct)	(2007 Sep)
Outburst onset (MJD)	$53430.7^{+1.2}_{-0.7}$	53637 ± 2	54259 ± 1	54352^{+8}_{-2}	54345 ± 3
Transition time (MJD)	53434.5 ± 1.0	53650.5 ± 1.0	54271.0 ± 0.5	54393.0 ± 0.5	54353.5 ± 2.5
Last hard state					
time (MJD)	53433.5 ± 0.5	53649.5 ± 0.5	54270.5 ± 0.5	54392.5 ± 0.5	54350.5 ± 0.5
Hardness ratio	0.7 ± 0.4	1.0 ± 0.3	1.50 ± 0.09	1.00 ± 0.05	1.3 ± 0.5
Luminosity	0.3 ± 0.2	0.45 ± 0.02	0.85 ± 0.04	1.11 ± 0.03	0.20 ± 0.03
First soft state					
time (MJD)	53435.5 ± 0.5	53651.5 ± 0.5	54271.5 ± 0.5	54393.5 ± 0.5	54355.5 ± 0.5
Hardness ratio	0.12 ± 0.03	0.13 ± 0.06	0.12 ± 0.01	0.10 ± 0.03	0.2 ± 0.1
Luminosity	0.75 ± 0.04	1.17 ± 0.02	2.00 ± 0.05	2.07 ± 0.05	0.74 ± 0.04
Pre-transition time (days)	$3.8^{+1.7}_{-2.2}$	13.5 ± 3	12 ± 1.5	$41^{+2.5}_{-8.5}$	8.5 ± 5.5
Transition luminosity	0.6 ± 0.2	0.8 ± 0.4	1.4 ± 0.6	1.6 ± 0.5	0.5 ± 0.3
Soft/Hard state at 15–50 keV max.	soft state	hard state	hard state	hard state	hard state
Type	F	S	S	S	S

* The same table as table 1 but for ASM and BAT data.

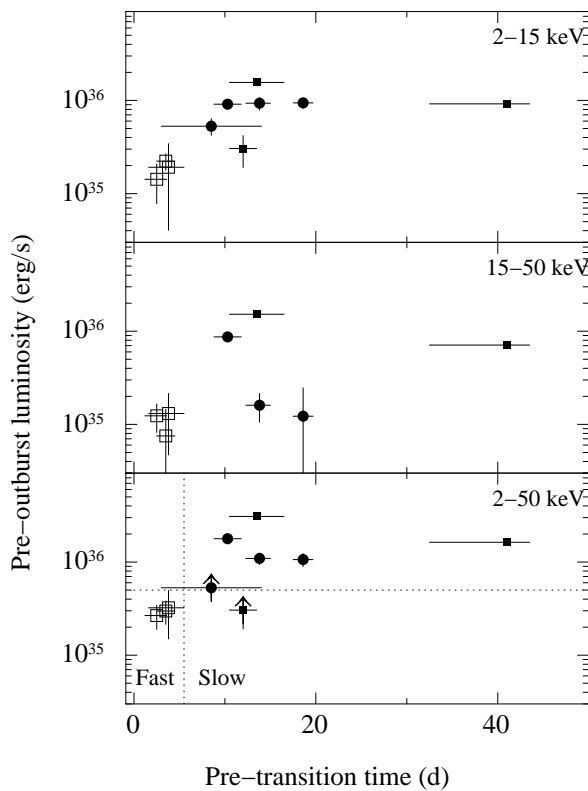


Fig. 6. Relation between pre-outburst luminosity in 2–15 keV (top), 15–50 keV (middle), 2–50 keV (bottom) and “pre-transition time”. The errors in “pre-transition time” are obtained in the same manner as in table 1. The errors in “pre-outburst luminosity” are $1\text{-}\sigma$ errors (cf. footnote 5). Squares are for 4U 1608–52 and circles for Aql X-1. Filled and open marks represent S-type and F-type, respectively.

scale. Figure 6 shows the correlations of the 2–15 keV luminosity by GSC or ASM, the 15–50 keV luminosity by BAT, and their sum of the 2–50 keV band to the pre-transition time. For the five outbursts observed with both the GSC and the ASM after the MAXI started the operation, we calculated pre-outburst luminosities in 2–15 keV band for both instruments and confirmed that the results are consistent with each other. Here, we employ GSC data because the statistical accuracy of the GSC data is better than that of the ASM. The pre-outburst luminosity of S-type tends to be higher than that of F-type.

In the middle panel of figure 6, two data points (4U 1608–52 outbursts in 2007 June and Aql X-1 outburst in 2007 September) are not plotted because the public BAT light curves during these two outbursts have data gaps or data points with negative count rates. Therefore, the average luminosities were not able to be obtained. Although these data are omitted in the middle panel we showed them in the bottom panel using the lower limits.

Finally, We examined the correlation between the transition luminosity (tables 1 and 2) and the pre-transition time. Figure 7 shows the obtained relation. The F-type points are in the left-down section while S-type points locate in the right-upper section. The transition luminosity of S-type is larger than that of F-type.

3. Discussion

We analyzed the initial rising behaviors of ten outbursts from Aql X-1 and 4U 1608–52 using data taken by MAXI/GSC, Swift/BAT, and RXTE/ASM. We have found the two types of hard-to-soft state transitions. One type behaves as the 15–50 keV intensity reaches the maximum before the hard-to-soft transition, and the other type does after the transition. There is a difference in the duration of the initial hard state, from the outburst onset to

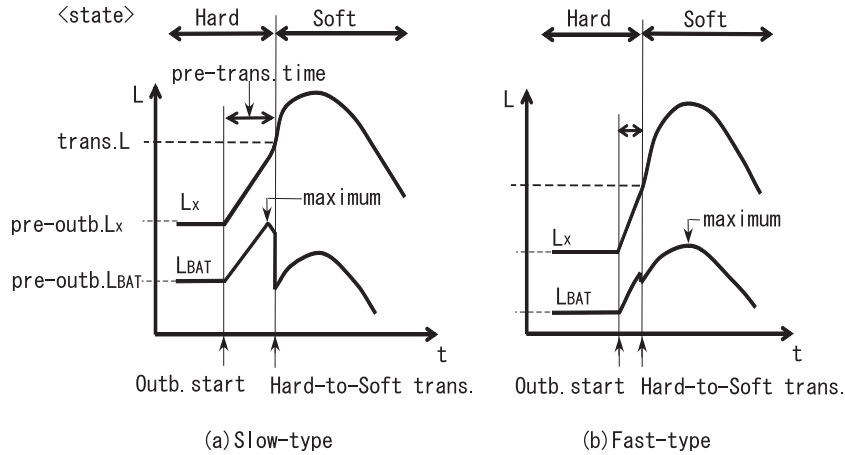


Fig. 8. Schematic drawings of 2–15 keV and 15–50 keV light curves (L_X and L_{BAT}) in each of S-type and F-type outbursts. Four differences in pre-transition time, transition luminosity, pre-outburst luminosity, and location of the 15–50 keV maximum luminosity between the S-type and the F-type are illustrated.

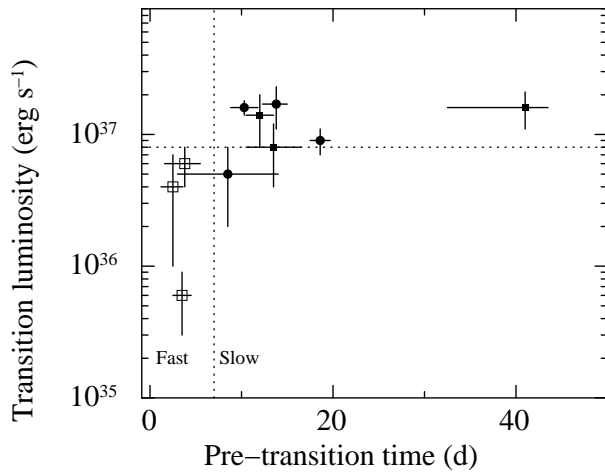


Fig. 7. Relation between transition luminosity and pre-transition time. The errors are obtained in the same manner as in table 1. Symbols are the same as those of figure 6.

the hard-to-soft transition. The durations of seven outbursts were longer than ~ 9 d, while the other three ones were shorter than that. Therefore we named the former type as slow-type (S-type) and the latter type as fast-type (F-type). These two types show the different properties in the following four points: (1) the duration from the outburst onset to the hard-to-soft transition (“pre-transition time”) in the S-type is longer than that in the F-type; (2) the 2–15 keV luminosity at the hard-to-soft state transition (“transition luminosity”) in the S-type is larger than that in the F-type; (3) the 15–50 keV luminosity reaches its maximum during the hard state in the S-type but during the soft state in the F-type; and (4) the luminosity before the outburst onset (“pre-outburst luminosity”) in the S-type is larger than in the F-type. Figure 8 illustrates the schematic light curves of the S-type and the F-type rising behaviors. We here discuss how and why two types

of the outburst rising are created and evolved.

The difference between the S-type and the F-type begins with the pre-outburst luminosity. We consider the irradiation on the accretion disk during the pre-outburst period as a key factor to separate the S-type from the F-type. The hard-to-soft state transition is generally considered as the transition of the accretion disk according to the change of the accretion rate (e.g., Mineshige & Wheeler 1989; Abramowicz et al. 1995). The X-ray irradiation on the disk from inner regions can affect the disk structure (Kim et al. 1999; Dubus et al. 2001, and referenced therein). If mass accretion from the companion star increases, the accretion disk is usually cooled down by the increased thermal soft X-ray emission. As the result, the geometrically thick disk turns to the thin disk, which corresponds to the hard-to-soft state transition. If an intense disk irradiation exists, the thick-to-thin disk transition is suppressed because the irradiation heats up the disk and keep the geometrically thick structure. Therefore, the pre-transition time becomes longer. This agrees with the observed feature that the pre-transition time in the S-type is longer than that in the F-type.

The source of the irradiation emission has several candidates such as blackbody emissions from the surface of the neutron-star and/or Comptonized emissions from the corona somewhere around the disk. The long pre-transition time is considered to cause the large “transition luminosity” in the S-type. The present results show that the S-type transition tends to occur at higher luminosity than the F-type transition does. Most of the S-type transitions occurred at the higher than 4% of the Eddington luminosity for $1.4M_{\odot}$. The different transition luminosity between the S-type and the F-type reminds us of a hysteretic behaviour in the state transition that has been reported in both BH-LMXBs and NS-LMXBs (Miyamoto et al. 1995; Maccarone & Coppi 2003; Yu et al. 2004). We thus consider that these root causes have some relation. Yu, van der Klis, and Fender (2004) proposed a “two-accretion-flow geometry” to explain the hysteresis.

According to their model, in case of the S-type, a sub-Keplerian flow (i.e., corona) may be initially irradiated by the pre-outburst radiation, and then the disk would be heated up to prevent a transition. To explain this behavior furthermore, theoretical calculations considering magneto-hydro dynamics are required, similar to those for BH-LMXB disks introduced by Oda et al. (2010).

In the S-type, the 15–50 keV luminosity gets the maximum during the initial hard state, whereas it does after the hard-to-soft transition in the F-type. The difference can be explained by the different values in the transition luminosity as follows. Both the 2–15 keV and 15–50 keV luminosities change similarly before/after the state transition. The 15–50 keV luminosity drops at the hard-to-soft transition in both the S-type and the F-type, although the drop is small in the F-type. In the S-type, the transition luminosity is relatively bright and the 15–50 keV luminosity drops so greatly at the transition that it will never recover to the level of the pre-transition period during the soft state. On the other hand, in the F-type, the transition luminosity is relatively faint and the drop at the transition is so small that both the 2–15 keV and the 15–50 keV luminosities reach the maximum after the transition.

The present results also resemble the hard-to-soft transition behavior in BH-LMXBs reported by Gierliński and Newton (2006). They obtained two types of transitions classified into the bright/slow or the dark/fast in the initial part of their outbursts. The bright/slow transition occurs at $\sim 30\%$ of the Eddington luminosity and takes $\gtrsim 30$ d during which the source quickly reaches the intermediate/very high state and then proceeds to the soft state at slower pace. The dark/fast is less luminous ($\lesssim 10\%$ of the Eddington luminosity), shorter ($\lesssim 15$ d) period, and the source does not slow its transition rate before reaching the soft state. It is quite similar to our results of NS-LMXBs in a point that there are two types of transitions in the initial part of the outbursts.

However, the parameters representing the transition duration are not exactly the same. We employed the “pre-transition time” from the outburst onset to the hard-to-soft transition for this, whereas Gierliński and Newton (2006) defined it by the period from the last hard-state time to first soft-state time and referred it as the “transition duration”. As for NS-LMXBs, the “transition duration” is very short ($\lesssim 1$ d) in most outbursts, and their difference cannot be recognized from the daily light curve. However, they are common in a point that the two types are different in the transition luminosity. Gierliński and Newton (2006) speculated that the distinction of the two types is due to irradiation and evaporation of the disk. Hence, we note that the behavior of outbursts of BH-LMXBs is similar to those of NS-LMXBs.

We have found two distinct groups of the fast and slow types in the outburst initial behavior from the data of only two soft transients, Aql X-1 and 4U 1608–52. It is a future issue whether the present result is common to general soft X-ray transients containing a neutron-star. Therefore, we expect that one pays attention to generalize the present result.

The authors would like to acknowledge the MAXI team for MAXI operation and for watching and analyzing real time data. They also thank the RXTE-ASM team and the Swift-BAT team for providing excellent data publicly. This research was partially supported by the Ministry of Education, Culture, Sports, Science and Technology (MEXT), Grant-in-Aid for Science Research 20244015.

Appendix. Outburst Onset

We define the outburst onset as the start point of the increase towards the outburst peak. We estimated the outburst onset from the GSC or ASM light curves with a 1-day time bin. We fitted the light curves around outburst onset with a model of two exponential functions. When the persistent component was constant within the error, we used a model with one constant and one exponential function. We determined the cross point of these two functions as the outburst onset. The errors are at the 90 % confidence level. In the cases of the outbursts of 4U 1608–52 in 2007 October and Aql X-1 in 2010 September, probably due to the variable persistent flux, the best-fit models are not formally acceptable. We estimated the errors in consideration of the fitting range. We explain how the outburst began in each outburst below.

4U 1608–52, 2010 March (figure 9a): The flux before outburst onset stayed in the almost constant level. After MJD=55256.5 (last hard state), the flux increased clearly, and next data point is “first soft state”. Thus, we determined the “last hard state” as the “outburst onset”.

4U 1608–52, 2011 March (figure 9b): The flux before outburst onset stayed in the almost constant level. We fitted a model with one constant and one exponential function between MJD=55600 and MJD=55644.

Aql X-1, 2009 November (figure 9c): The flux decreased between MJD \sim 55130 and \sim 55140. After that, the flux increased towards the peak of the outburst. We fitted a model with two exponential functions between MJD=55131 and MJD=55153.

Aql X-1, 2010 September (figure 9d): The flux decreased between MJD \sim 55248 and \sim 55440. After that, the flux increased towards the peak of the outburst. We fitted a model with two exponential functions between MJD=55428 and MJD=55451. However, because the slope changed during the increase, the fit is not acceptable. We estimated the errors in consideration of the change of slope.

Aql X-1, 2011 October (figure 9e): The flux decreased between MJD \sim 55835 and \sim 55845. After that, the flux increased towards the peak of the outburst. We fitted a model with two exponential functions between MJD=55835 and MJD=55856.

4U 1608–52, 2005 March (figure 10a): The flux before outburst onset stayed in the almost constant level. We fitted a model with one constant and one exponential function between MJD=53390 and MJD=53435.

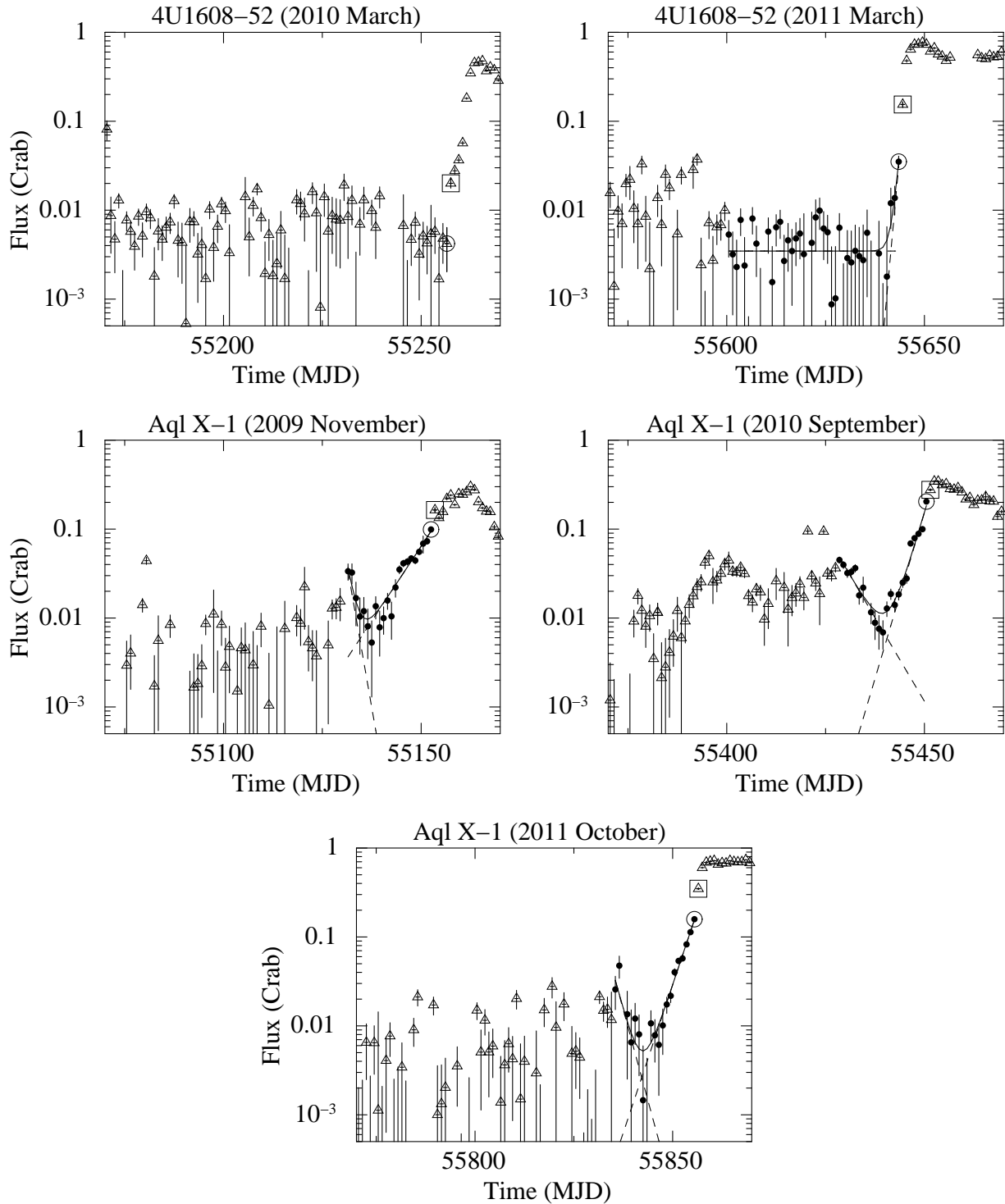


Fig. 9. MAXI-GSC light curves (2–20 keV) of five outbursts around the onset fitted with two exponential functions. The solid curve shows the best-fit model. The dashed lines show each components. Filled circles represent data points used for the model fit. Open circles indicate the data point of “last hard state”. Open squares indicate the data point of “first soft state”.

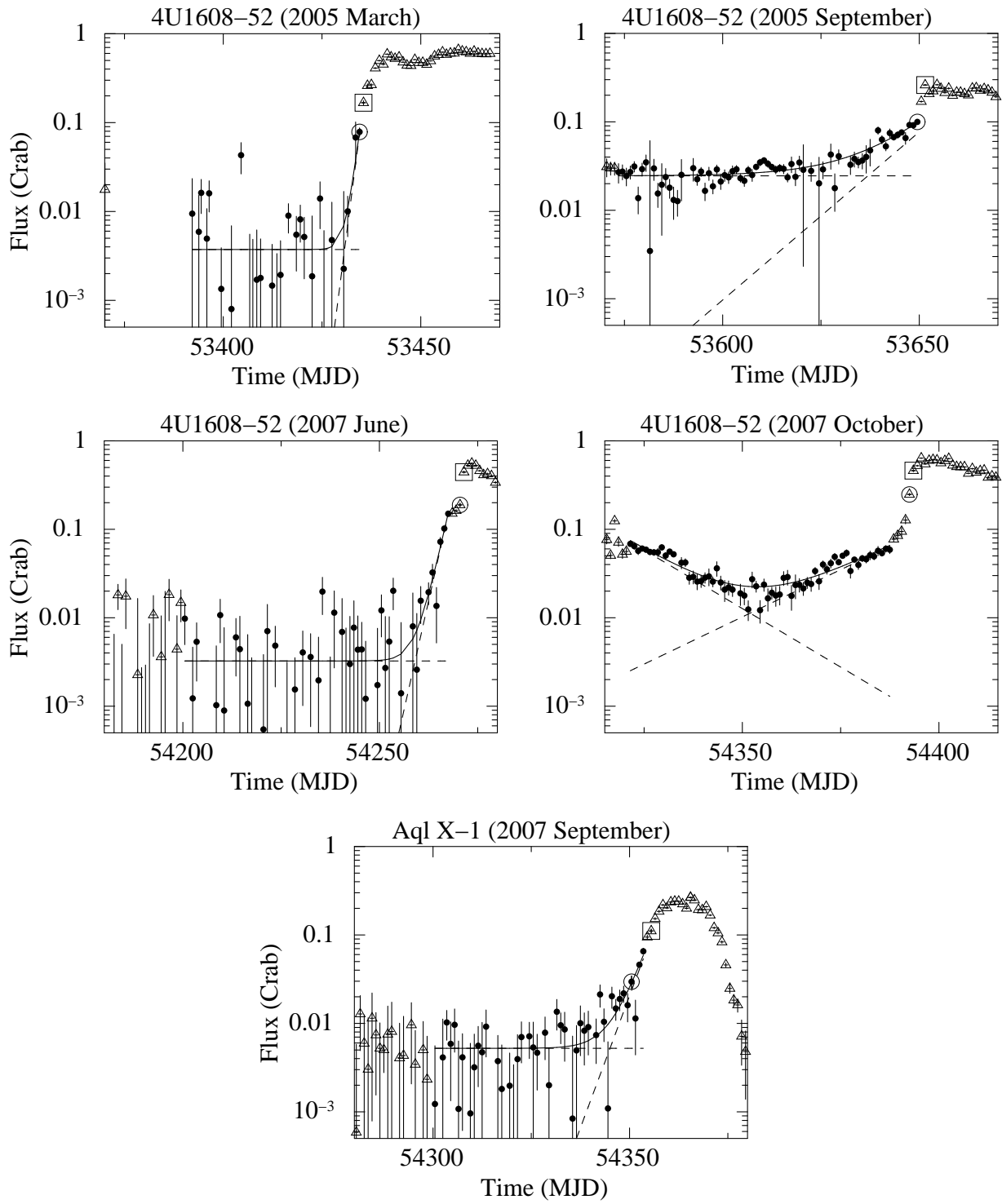


Fig. 10. RXTE-ASM light curves (2–10 keV) of five outbursts around the onset fitted with two exponential functions. Marks are the same as in figure 9.

- 4U 1608–52, 2005 September (figure 10b):** The persistent trend before outburst onset was considered to stay in the almost constant level, although the flux is variable. We fitted a model with one constant and one exponential function between MJD=53573 and MJD=53650.
- 4U 1608–52, 2007 June (figure 10c):** The flux before outburst onset stayed in the almost constant level. We fitted a model with one constant and one exponential function between MJD=54200 and MJD=54268.
- 4U 1608–52, 2007 October (figure 10d):** The flux decreased between MJD~54320 and ~54350. After that, the flux increased towards peak of the outburst. We fitted a model with two exponential functions between MJD=54321 and MJD=54388. However, because the slope changed during the increase, the fit is not acceptable. We estimated the errors in consideration of the change of inclination.
- Aql X-1, 2007 September (figure 10e):** The flux before outburst onset stayed in the almost constant level. We fitted a model with one constant and one exponential functions between MJD=54300 and MJD=54354.

References

- Abramowicz, M.A., Chen, X., Kato, S., Lasota, J., & Regev, O. 1995, *ApJ*, 438, L37
- Barret, D. 2001, *Adv. Space Res.*, 28, 307
- Barthelmy, S. D., et al. 2005, *Space Sci. Rev.*, 120, 143
- Bradt, H. V., Rothschild, R. E., & Swank, J. H. 1993, *A&AS*, 97, 355
- Campana, S., Colpi, M., Mereghetti, S., Stella, L., & Tavani, M. 1998 *A&A Rev.*, 8, 279
- Chen, X., Zhang, S. H., & Ding, G. Q. 2006, *ApJ*, 650, 299
- Dubus, G., Hameury, J. -M., & Lasota, J. -P. 2001, *A&A*, 373, 251
- Farinelli, R., Titarchuk, L., Paizis, A., & Frontera, F. 2008, *ApJ*, 680, 602
- Galloway, D. K., Munro, M. P., Hartman, J. M., Psaltis, D., & Chakrabarty, D. 2008, *ApJS*, 179, 360
- Gehrels, N., et al. 2004, *ApJ*, 611, 1005
- Gierliński, M., & Done, C. 2002, *MNRAS*, 337, 1373
- Gierliński, M., & Newton, J. 2006, *MNRAS*, 370, 837
- Hasinger, G. & van der Klis, M. 1989, *A&A*, 225, 79
- Homan, J. et al. 2001, *ApJS*, 137, 377
- Homan, J. et al. 2010, *ApJ*, 719, 201
- Kim, S.-W., Wheeler, J.C., & Mineshige, S. 1999, *PASJ*, 51, 393
- Kirsch, M. G., et al. 2005, *Proc. SPIE*, 5898, 22
- Kitamoto, S., Tsunemi, H., & Miyamoto, S. 1993, *ApJ*, 403, 315
- Koyama, K. et al. 1981, *ApJ*, 247, L27
- Levine, A. M., Bradt, H., Cui, W., Jernigan, J. G., Morgan, E. H., Remillard, R., Shirey, R. E., & Smith, D. A. 1996, *ApJ*, 469, L33
- Lin, D., Remillard, R. A., & Homan, J. 2007, *ApJ*, 667, 1073
- Maccarone, T. J. 2003, *A&A*, 409, 697
- Maccarone, T. J., & Coppi, P.S. 2003, *MNRAS*, 338, 189
- Matsuoka, M., et al. 2009, *PASJ*, 61, 999
- Mihara, T., et al. 2011, *PASJ*, 63, S623
- Mineshige, S., & Wheeler, J.C. 1989, *ApJ*, 343, 241
- Mitsuda, K., et al. 1984, *PASJ*, 36, 741
- Mitsuda, K., Inoue, H., Nakamura, N., & Tanaka, Y. 1989, *PASJ*, 41, 97
- Miyamoto, S., Kitamoto, S., Hayashida, K. & Egoshi, W. 1995, *ApJ*, 442, L13
- Morii, M. 2010, *Astronoma. Telegram*, 2462
- Nakamura, N., Dotani, T., Inoue, H., Mituda, K., & Tanaka, Y. 1989, *PASJ*, 41, 617
- Negoro, H., et al. 2010, *ASPC*, 434, 127N
- Oda, H., Machida, M., Nakamura, K. E., & Matsumoto, R. 2010, *ApJ*, 712, 639
- Paizis, A., et al. 2006, *A&A*, 459, 187
- Raichur, H., Misra, R., & Dewangan, G. 2011, *MNRAS*, 416, 637
- Remillard, A., & McClintock, J. E. 2006, *ARA&A*, 44, 49
- Sakurai, D., Yamada, S., Torii, S., Noda, H., Nakazawa, K. & Makishima, K. 2012, *PASJ*, in press
- Šimon, V. 2002, *A&A*, 381, 151
- Šimon, V. 2004, *A&A*, 418, 617
- Smith, D. M., Heindl, W. A., & Swank, J. 2002, *ApJ*, 569, 362
- Sugizaki, M., et al. 2011a, *PASJ*, 63, S635
- Sugizaki, M., et al. 2011b, *Astronomer's Telegram*, 3237
- Takahashi, H., Sakurai, So., & Makishima, K. 2011, *ApJ*, 738, 62
- Tang, J., Yu, W., & Yan, Z. 2011, *Research in Astron. Astrophys.*, 11, 434
- Tomida, H., et al. 2011, *PASJ*, 63, 397
- van der Klis, M. 1994, *ApJS*, 92, 511
- White, N. E., Stella, L., & Parmar, A. N. 1988, *ApJ*, 324, 363
- Yamaoka, K., et al. 2011, *Astronomer's Telegram*, 3686
- Yu, W., & Dolence, J. 2007, *ApJ*, 667, 1043
- Yu, W., van der Klis, M. & Fender, R. 2004, *ApJ*, 611, L121
- Yu, W., & Yan, Z. 2009, *ApJ*, 701, 1940